CRITICAL RAW MATERIAL ELECTROCATALYSTS REPLACEMENT
ENABLING DESIGNED POST-2020 PEMFC

Grant agreement no.: 779366
***Start date**: 01.01.2018 – **Duration**: 36 months*
***Project Coordinator**: Deborah Jones – CNRS*

DELIVERABLE REPORT

DELIVERABLE D2.2 – REPORT ON THE BENCHMARKING OF INTERNATIONAL STATE-OF-THE-ART NON-PGM CATALYSTS AND/OR CCMS	
Due Date	30th September 2018
Author (s)	Alin Orfanidi (BMW), Nicolas Donzel (CNRS), Jonathan Sharman (JMFC), Alex Martinez Bonastre (JMFC), Frederic Jaouen (CNRS)
Workpackage	WP2
Workpackage Leader	BMW
Lead Beneficiary	BMW
Date released by WP leader	18th October 2018
Date released by Coordinator	18th October 2018

DISSEMINATION LEVEL		
PU	*Public*	***X***
PP	*Restricted to other programme participants (including the Commission Services)*	
RE	*Restricted to a group specified by the consortium (including the Commission Services)*	
CO	*Confidential, only for members of the consortium (including the Commission Services)*	

NATURE OF THE DELIVERABLE		
R	*Report*	***x***
P	*Prototype*	
D	*Demonstrator*	
O	*Other*	

SUMMARY	
Keywords	*Benchmark of commercial PGM-free CCMs, ex-situ characterization of SoA Fe-N-C catalysts*
Abstract	*The results of benchmarking the performance of commercial PGM-free based CCMs are presented. The results are in good agreement between different partners, despite the use of different testing hardware. The commercial PGM-free CCMs exhibit lower performance than the project performance targets providing 0.15 A/cm^2 @ 0,418 V under operating mode 3, while the performance target is 0.6 A/cm2 @ 0,71 V. This report also provides the results of ex situ RDE electrochemical characterisation of the commercial Fe-N-C catalyst.*
Public abstract	*The results of benchmarking the performance of commercial PGM-free based CCMs are presented. The results are in good agreement between different partners, despite the use of different testing hardware. The commercial PGM-free CCMs exhibit lower performance than the project performance targets providing 0.15 A/cm^2 @ 0,418 V under operating mode 3, while the performance target is 0.6 A/cm2 @ 0,71 V. This report also provides the results of ex situ RDE electrochemical characterisation of the commercial Fe-N-C catalyst.*

REVISIONS			
Version	**Date**	**Changed by**	**Comments**
0.3	18.10.2018	Alin Orfanidi	draft
0.3	18.10.2018	Deborah Jones	Minor edits, finalisation

DELIVERABLE TITLE

CONTENTS

1. INTRODUCTION

The objective of task 2.3 in WP2 is to gain a deeper understanding and an overall picture of the performance and durability of current best-in-class non-PGM catalysts and how far away these materials are from the CRESCENDO performance target (600 mA/cm²@0.7 V; ~ 0.42 W/cm² under the harmonised European automotive reference conditions).

For the benchmarking, ex situ rotating disc electrode electrochemical characterisation (RDE) of catalysts available at laboratory scale as well as industrial scale were tested, including those from CNRS, ICL, University of New Mexico, and Pajarito Powder. The original plan was that the most active material from the RDE testing would be used to prepare laboratory scale CCMs for fuel cell testing and to then compare the performance of the latter with CCMs made from Pajarito Powder's catalyst. However, as will be shown in section 3.7, the Pajarito Powder catalyst had an ORR activity measured in RDE closely matching the most active laboratory scale catalysts benchmarked in CRESCENDO, and since BMW had already purchased commercial CCMs containing this material, it was decided to only test the commercially available ones.

BMW purchased commercially available non-PGM CCMs from Pajarito Powder (manufactured by EWii), distributed them between CNRS, ICL and JMFC, and BMW, CNRS and JMFC tested them in single cells. Due to the poor performance of the commercial non-PGM CCMs in laboratory scale MEAs, automotive size testing was not performed.

2. EXPERIMENTAL

2.1 SPECIFICATIONS OF COMMERCIALS PGM-FREE CCMS

Commercially available PGM-free CCMs were purchased from Pajarito Powder (manufactured by EWII). The CCM specifications are listed in the table below:

Anode Pt loading [mg_{Pt}/cm^2]	0.1
Cathode Fe-N-C catalyst loading [mg_C/cm^2]	3.0
Electrode active area [cm^2]	7.1 x 7.1
PEM area [cm^2]	9.1 x 9.1
PEM type	LYT0008
GDL 29BC thickness [µm]	235-250

The CCM configuration that was received for testing is depicted in Figure 1c. There was no sub-gasket on the CCM (3 layer CCM).

Figure 1 depicts the Pajarito Powder CCM without a sub-frame (as received).

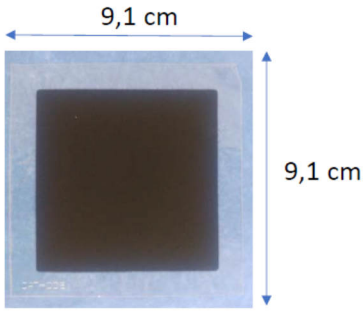

Figure 1. Pajarito CCM with no sub-frame.

2.2 SCREENER CELLS FOR SUBSCALE SINGLE CELL TESTING AND COMMERCIALS CCMS

The screener single cells (43,56 cm^2 or 50 cm^2) that were used by each partner (JMFC, CNRS and BMW) for the benchmarking of the Pajarito Powder CCMs is described in this section.

Since all the screener cells used had different flow field channel geometry and cell area, different performance was expected, especially at high current densities and/or in wet conditions. For this reason, it is of great importance to describe in detail the cells used for the benchmarking process.

a. CNRS screener cells

The screener cells from CNRS use a soft-sealing concept, where the compression of the MEA is defined by the applied force/torque on the cell hardware.

Table 1. The CNRS cell specifications.

Type of Specification	Cell Configuration #2
Flow field type	Parallel
Monopolar plate size (cm x cm)	10 x 10
Material of Flow field	Gold coated
Heating type	Electric
Sealing type	Soft sealing
Controlling cell compression	Torque

b. BMW screener cell

The screener cell BMW used was a modified TP50 purchased from TandemTech. This cell uses a hardstop sealing concept, where the compression of the MEA is controlled by the height of the seal and is not dependent on the clamping pressure of the cell hardware. The clamping pressure required to seal the cell from external leakage is 9 bara. The GDL compression was set to 20% for all experiments by using incompressible fibre glass-reinforced PTFE-gaskets with the appropriate thickness. Fuel cell tests were

performed on an automated FuelCon fuel cell test station. Figure 2 depicts the cell type and flow field used, as well as the framing of the 50 cm^2 CCMs from Pajarito Powder CCMs with a sub-frame, which reduced the active area to 43.56cm^2.

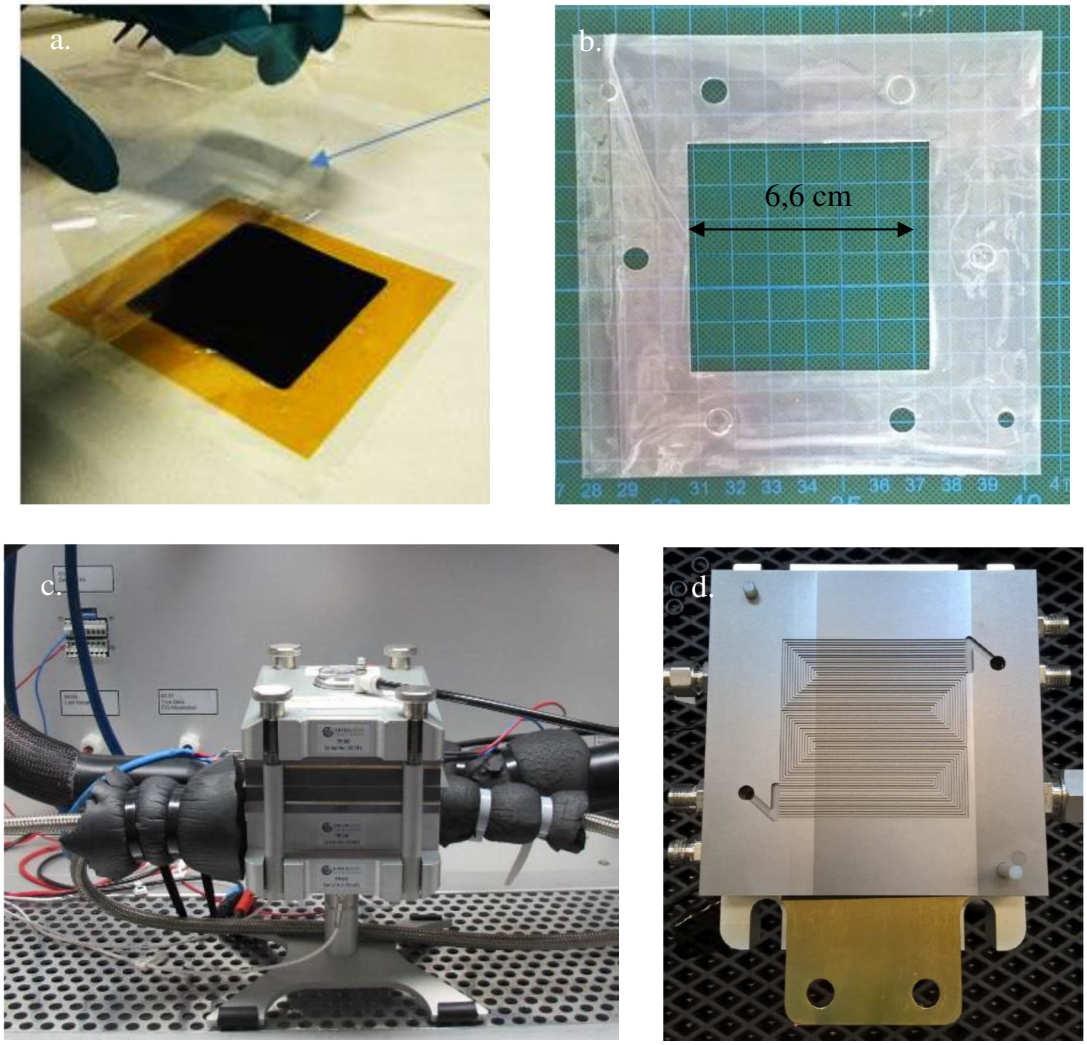

Figure 2 a. Framing the Pajarito CCM in PEN subgasket and b. PEN Subgasket with an active area window of 43.56 cm^2, c. BMW subscale single cell hardware configuration and d. the 50 cm^2 flow field

Table 2. The BMW cell specifications

Type of Specification	Cell Configuration
Flow field type	14 channel serpentine, both anode and cathode
Monopolar plate size (cm x cm)	13 x 13
Material of Flow field	Graphite composite
Heating type	Liquid medium
Sealing type	Hard-stop
Controlling cell compression	Pressurised piston

c. JMFC screener cell

Figure 3 shows the cell type and flow field used by JMFC for testing Pajarito Powder. The active area was 50 cm^2.

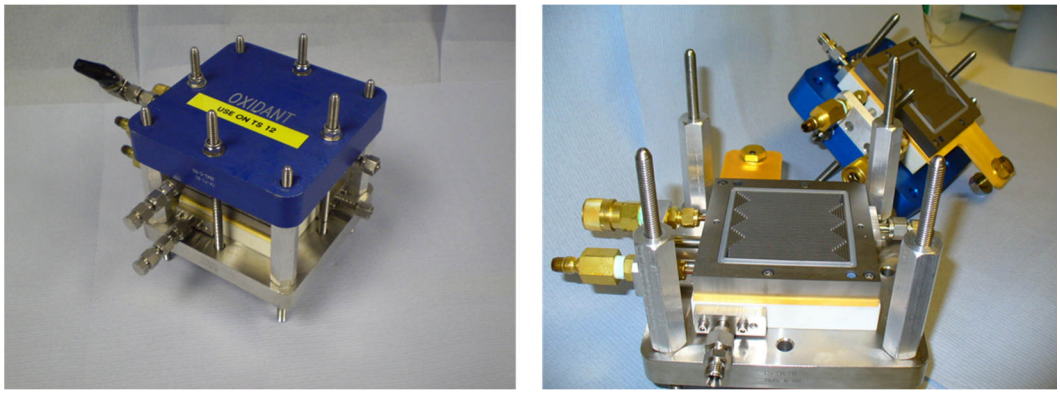

Figure 3. JMFC subscale single cell hardware configuration.

Table 3. The JMFC cell specifications.

Type of Specification	Cell Configuration
Flow field type	Anode 2 channel serpentine, cathode 3 channel serpentine
Monopolar plate size (cm x cm)	Plate 10.2 x 10.2, Flow-field 7.4 x 7.4
Material of Flow field	Graphite composite (pyrolytic surface treatment)
Heating type	Liquid medium
Sealing type	Rubber gasket
Controlling cell compression	gas piston

2.3 ACTIVATION AND PERFORMANCE PROTOCOLS

- **BMW testing protocol:**

Conditioning: All MEAs were conditioned before testing using the same voltage controlled loop with H_2/air flows of 1,5/3,3 Nl/min at 80 °C, 100 % relative humidity, and 170 $kPa_{abs,inlet}$ consisting of holds at 0.7 V for 10 min and 0.4 V for 10 min, this sequence was repeated until stable performance was obtained.

Polarisation curves: Stoichiometric-flow H_2/air (s=1.5/2.0) and H_2/O_2 (s=2.0/9.5) polarisation curves were recorded in current-controlled mode at 230 kPa_{abs} outlet pressure, with both reactants humidified to the

same relative humidity (RH). The polarisation curves were recorded from low to high current densities; each current density point was held for 5 min and the resulting voltage was averaged over the final 30 s. At each current density, the respective high frequency resistance was recorded using a Hioki at 1 kHz.

- **CNRS testing protocol:**

Conditioning: Two different conditioning/activation protocols were used.

a. A repeated loop with H_2/air flows of 2.0/2.0 Nl/min at 80 °C, 100 % relative humidity, and 170 $kPa_{abs,outlet}$ with holds at 0.8 V for 10 min and 0.4 V for 10 min. This sequence was repeated until stable performance was obtained.
b. A steady state hold at 0.55V for 3.5 hours with H_2/air flows of 2.0/2.0 Nl/min at 80 °C, 100 % relative humidity and 170 $kPa_{abs,outlet}$.

Polarisation curves: Stoichiometric-flow H_2/air (s=1.5/2.0) and H_2/O_2 (s=2.0/9.5) polarization curves were recorded in current-control mode at 230 kPa_{abs} outlet pressure, with both reactants humidified to the same relative humidity (RH). The polarisation curves were recorded from low to high current densities; each current density point was held for 5 min and the resulting voltage was averaged over the final 30 s. At each current density, the respective high frequency resistance was managed and recorded by a built-in frequency response analyser from Biologic SP-150.

- **JMFC testing protocol:**

Conditioning: Table 4 shows the protocol used at JM for conditioning and testing Pajarito Powder CCMs. Initial conditioning was done under potentiostatic mode at 80 °C, 100 % relative humidity, and 170 kPa_{gauge_inlet} under H_2/air stoichiometry of 2.05/2.0 at 0.65 V.

Test	Anode Gas Composition	Anode Stoich	Cathode Gas Composition	Cathode Stoich	% RHA	% RHC	Anode Inlet P (kPag)	Cathode Inlet P (kPag)	Cell Temperature (deg C)	Current Density (mAcm-2)	Duration (hrs)
50cm2 Screener Cell Assembly											
Leak Testing											
Shorting Test (Agilent)											
1) Low Potential Voltage Hold	H2	2.0	Air/Oygen	2.0-10.0	100	100	170	170	80	0.65V Hold	
2) 3-Way-Ox	H2	2.0	Air/Helox/O2	2/2/10	100	100	170	170	80	50-2000	
3) Reconditioning	H2	2.0	Air	2.0	100	100	50	50	80	500	1hr
4) Oxygen polar	H2	2.0	Oxygen	10.0	100	100	50	50	80	50-1500	
7) Conditioning	H2	2.0	Air	2.0	30	30	170	170	80	500	5hr
8) 3-Way-Ox	H2	2.0	Air/Helox/O2	2/2/10	30	30	170	170	80	50-2000	
9) Temperature Sweep	H2	2.0	Air	2.0	(53DP)	(53DP)	170	170	30-90-30	100 200 500	
10) Reconditioning	H2	2.0	Air	2.0	100	100	100	100	80	500	1hr
Cathode CV	H2	N/A	N2 - N2/CO	N/A	100	100	100	100	80	N/A	

Polarisation curves: After conditioning, a set of polarisation curves was performed as described in Table 4. The cathode gas was switched between air, helox (21% O_2 in He) and oxygen at a particular operating humidity, temperature and pressure. In addition, a temperature sweep was done after the polarisation curves in H_2/air. The protocol finished with a cyclic voltammogram on the cathode side.

2.4 Ex situ RDE electrochemical characterization methods for catalyst benchmarking

The electrochemical benchmark test consists of the determination of the catalytic activity via a rotating ring disk electrode set-up (RDE) at two different catalyst loadings on the electrode. Loadings of 0.8 mg cm^{-2} and 0.2 mg cm^{-2} were chosen to study the influence of layer thickness on the catalyst performance.

The four catalysts belong to the current best-in-class catalysts, denoted here as CNRS, ICL, PP and UNM, according to the catalyst origin. The first catalyst CNRS was prepared from ferrous salt, phenanthroline and ZIF-8, and pyrolysed in inert gas. It features mostly atomically-dispersed FeN_xC_y sites (68%) as Fe species, the remainder being metallic and metal-carbide Fe particles (see D3.1). The second catalyst, ICL, was prepared from the polymerisation of 1,5-diaminonaphthalene in presence of ammonium persulfate, forming self-assembled nanospheres which were pyrolyzed under inert gas. This catalyst features only atomically-dispersed FeN_xC_y sites as Fe species (see D3.1 and Ref. D. Malko, T.Lopes, E. Symianakis and A. Kucernak, J. Mater. Chem. A, 4 (2016) 142). The third catalyst, PP is the only commercially available non-PGM catalyst tested, produced by Pajarito Powder (NM, USA). It is prepared from a Fe salt, a source of nitrogen and carbon and using a silica hard-templating method to generate spherical mesopores after removal of silica by HF etching after the pyrolysis step. The Fe species in PP is mainly metallic and metal-carbide particles embedded in N-doped carbon matrix, along with a minority of atomically-dispersed FeN_xC_y sites (see D3.1). The fourth catalyst is from University of New Mexico (satellite partner of CRESCENDO) and was also prepared via a silica hard-templating method, but at smaller scale, resulting in most of the Fe being present as atomically-dispersed FeN_xC_y sites (89%) and a minority of Fe present as metallic and metal carbide particles embedded in N-doped carbon matrix (see D3.1).

- **Catalyst powder morphology**

No milling of the pyrolysed catalyst powders was applied systematically. However, if the average particle size measured with dynamic light scattering (DLS) was > 1 μm, then planetary ball milling with a zirconia vial and balls (400 rpm, 40 min, 5 mm zirconia balls, 50/50 IPA/water slurry) was applied and the DLS particle size measured again, with the aim of reaching an average particle size below 1 μm, more appropriate to prepare catalyst inks and to promote smooth and uniform RDE layers.

- **Ink formulation for RDE**

The catalyst ink consisted of a slurry of the catalyst made with isopropanol and ultrapure water in a mass ratio of 1:1 and Nafion (5 wt%, Sigma-Aldrich). The catalyst content was 0.5 wt% (0.2 mg cm^{-2} loading) and 2.0 wt% (0.8 mg cm^{-2} loading) of the total ink mass. The ionomer to catalyst ratio was 1:2. The slurry was ultra-sonicated until a stable suspension was reached.

- **Set-up**

The electrolyte was 0.5 M sulfuric acid (ANALR grade or EMSURE Merck Millipore, as available to the project partners). All the measurements were performed in a glass jacket cell at 25 °C with a reversible hydrogen electrode (RHE) reference electrode, a graphite counter electrode, and a glassy carbon disk as the working electrode. The concentric ring electrodes around the glassy carbon disk were made from platinum or gold. The disk electrodes were polished and cleaned in an ultra-sonication bath with isopropanol and ultrapure water. The cleaned electrodes were dried in nitrogen and the ink applied to the surface and dried in an oven at 50 °C, or at room temperature.

- **Break-in procedure**

The activation of the catalyst was performed in O_2-saturated electrolyte via cyclic voltammetry (0.0 V – 1.0 V_{RHE}, 10 mV s^{-1}) with a minimum of five cycles until the change in capacitance in the 0.95 – 1.0 V_{RHE} region between two successive scans was less than 2 %.

- **ORR activity measurement and H_2O_2 formation**

Cyclic voltammetry was performed in an O_2-saturated electrolyte (0.925 – 0.00 V_{RHE}, 1 – 2 mV s^{-1}, rotation 1600 rpm, ring potential held at 1.5 V_{RHE}) starting from open circuit potential (OCP) to the lower potential of 0.0 V_{RHE} and a back scan to 0.925 V_{RHE}.

- **Data Analysis**

For the determination of the kinetic current density j_{kin} the forward and back scans of the cyclic voltammetry of the disc current density were averaged to compensate for the capacitance, and the values of the current density j at 0.80 and 0.85 V_{RHE} and the diffusion limited current density j_{lim} at 0.20 V_{RHE} were determined. The Koutecký-Levich equation was used to calculate the kinetic current density at 0.80 and 0.85 V_{RHE}.

$$\frac{1}{j} = \frac{1}{j_{kin}} + \frac{1}{j_{lim}}$$

$$j_{kin} = \frac{j \cdot j_{lim}}{j_{lim} - j}$$

The following formula is used for the evaluation of the H_2O_2 production, with N as the collection efficiency of the ring -electrode.

$$\%H_2O_2 = \frac{2 \cdot I_{Ring}/N}{I_{Disk} + I_{Ring}/N} \cdot 100$$

3. Results and Discussions

3.1 Conditioning protocol of Pajarito Powder based CCMs

JMFC, CNRS and BMW used different activation protocols (as described in the experimental section). The behavior of the MEAs under these various conditions are depicted in Figure 4-5. In all Figures, it is apparent that the performance of the MEAs increases during the first ~20 min and thereafter starts decreasing rapidly. The increase in performance can be attributed to the hydration of the membrane and the catalyst layer (CL), as the HFR decreases over the first 20 min. However, the observed decrease of the performance can certainly not be attributed to deactivation/degradation of the catalyst. A working hypothesis, still not confirmed, is that the degradation was caused by flooding of the catalyst layer pores due to high relative humidity, inhomogeneous ionomer distribution and/or too high I/C and too thick a catalyst layer.

It is clear that the activation protocol for these type of MEAs does not seem to play a role with respect to the stability or performance after the first 20 min.

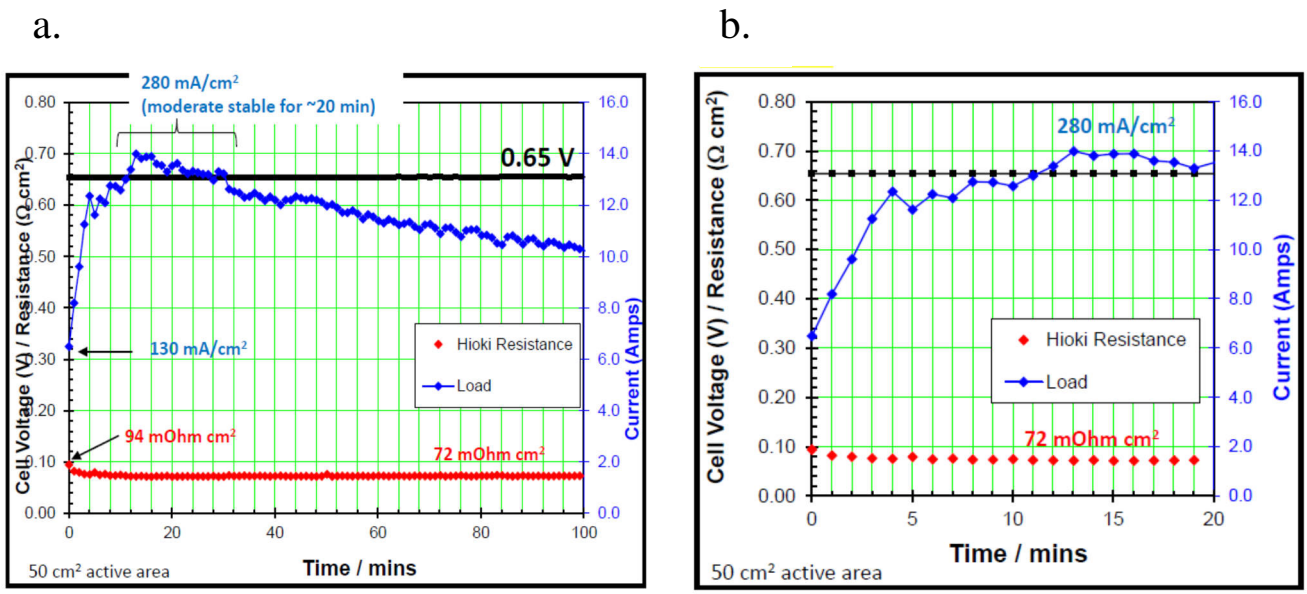

Figure 4 a. Conditioning of Pajarito CCMs from JMFC at 100% RH and 170kPa$_{,gauge\text{-}inlet}$ under H_2 and Air stoichiometry of 1.5 and 1.8 respectively, under constant voltage 0.65V and b. magnified portion of a.

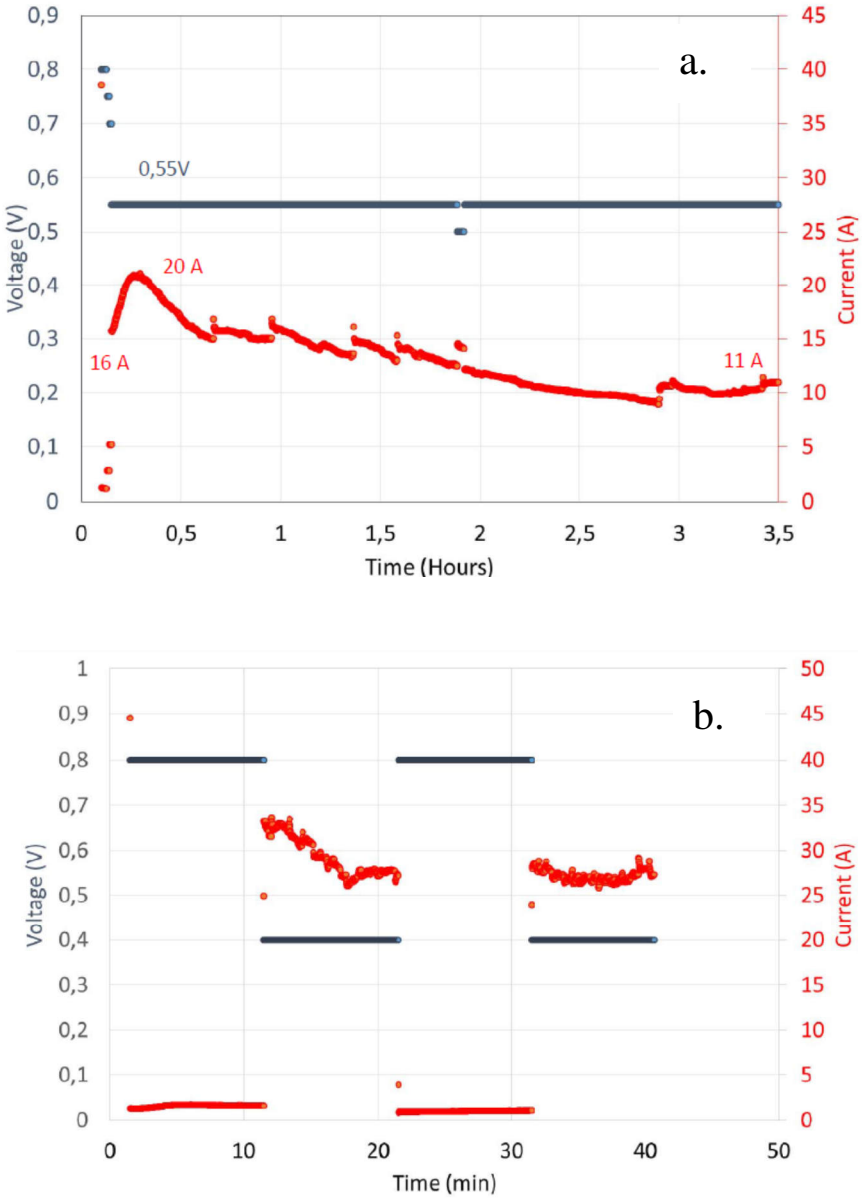

Figure 5. Conditioning of Pajarito Powder CCMs from CNRS a. Steady state holding at 0.55V for 3.5 hours with H2/air flows of 2.0/2.0 Nl/min at 80°C, 100 % relative humidity, and 170 kPaabs,outlet), b. A repetition loop with H2/air flows of 2.0/2.0 Nl/min at 80°C, 100 % relative humidity, and 170 kPa abs,outlet): 0.8 V for 10 min and 10 min at 0.4 V, this sequence was repeated until stable performance is acquired**.**

BMW observed the same behaviour as JMFC and CNRS.

3.2 Stability of Pajarito Powder Based CCMs and Performance

The stability of the Pajarito Fe-N-C catalyst based MEAs were evaluated by CNRS, JMFC and BMW.

CNRS used two different assembly torques to compress the cell, as described in detail in the section on the test hardware configuration. By increasing the applied torque the compression of the MEA increases

as well, as a soft sealing concept was being used. Figure 6 depicts the performance of 2 cells after the activation protocol and before the stability test. Each cell was assembled with a different torque.

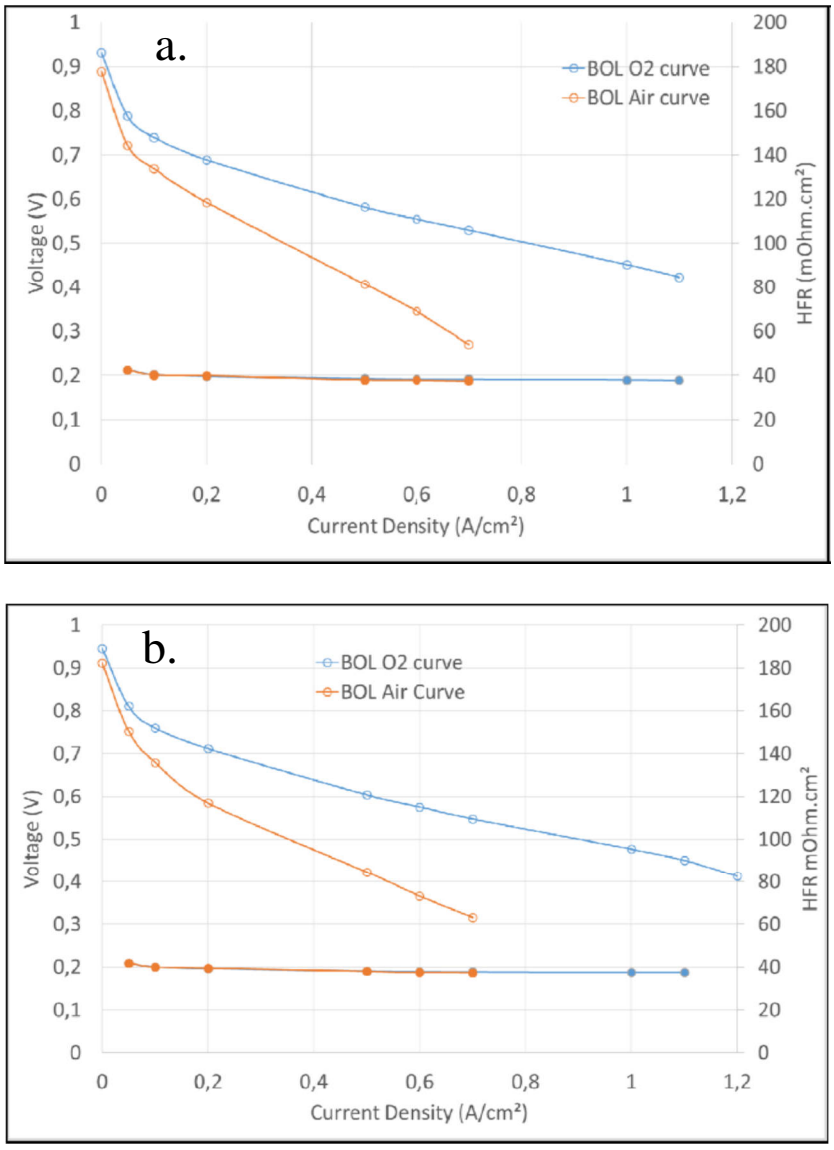

Figure 6. Performance curves under 100% RH and 2.3 bara under H_2 and O_2 stoichiometry of 2.0 and 9.5 respectively as well as H_2 and air stoichiometry of 1.5 and 2.0 respectively. The polarization curves were acquired before the stability test (BOL) with assembled torque: a. 3 Nm and b. 2 Nm.

The data in Figure 6 shows that there is no performance difference with respect to the assembly torque. In addition, the HFR in both cases is identical, indicating no change in contact resistance with the applied torque. However, it has to be pointed out that these MEAs also experienced different activation protocols, so comparison of the performance with respect to applied torque may not be definitive, as it is known that the activation protocol influences the overall MEA performance. This comment is applicable for Pt based MEAs but in non-PGM MEAs it might not be the case, as initial data suggests in section 3.1.

Figure 7 depicts the stability measurements obtained with applied torques of 3 Nm and 2 Nm at CNRS. When using the lower compression (i.e torque) the MEA performance is slightly higher at the beginning of the stability test and more stable compared to the higher assembly torque. For the MEA under higher

compression of 3 Nm, it was observed that the performance was oscillating and was very unstable, which might be indicative of blockage of the channels from water droplets due to intrusion of the GDL into the channels, or reduced GDL porosity due to over-compression of the MEA. In addition, the degradation rate was significantly higher at 3 Nm, where almost ~38% loss of the initial performance was lost within 18 hours of the stability test. In contrast, for the lower compression using a torque of 2 Nm, the performance loss was ~50% after 65 hours of continues operation (2.1% versus 0.8 % loss per hour).

After the stability test, the performance of the cell was not stable under current control mode. As a result, polarisation curves at the end-of-life of the MEA could not be recorded.

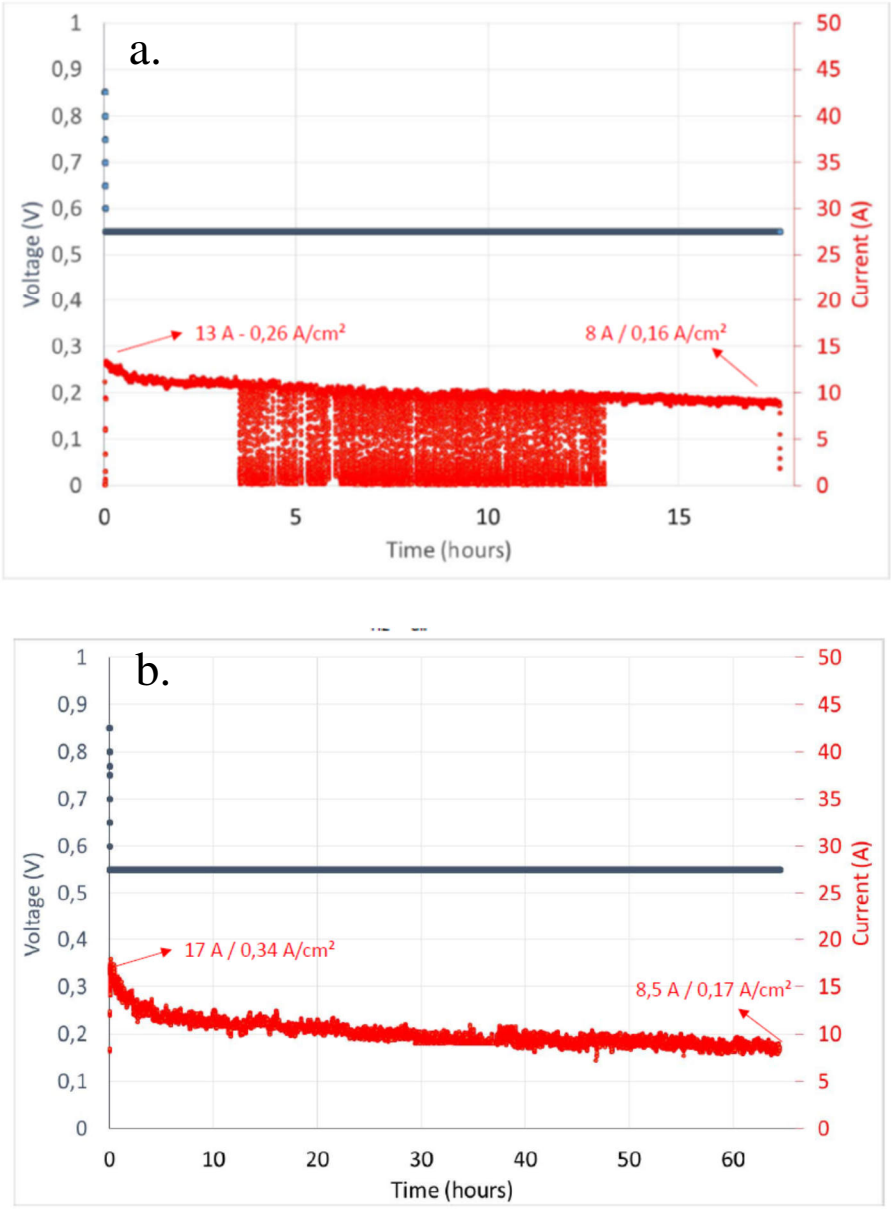

Figure 7. Stability test conducted at CNRS at 0.55V under 100% RH and 2.3 bara with a cell temperature of 80°C under stoichiometry of 1.5 for H_2 and 2.0 for air with assembled torque: a. 3 Nm and b. 2 Nm.

A similar degradation rate was observed when tested at BMW under the same experimental conditions as CNRS (Figure 7). To be more precise, after ~60 hours of continuous operation the performance loss was ~41% (Figure 8). It has to be stated that BMW used a fixed GDL compression of 20% and the compression with respect to CNRS may well have been different, which may have led to a difference in the degradation

rates. Due to the rapid performance losses, it is clear that any sensitivity analysis of these particular MEAs for pressure and air stoichiometry would have to be conducted within the first 5 hours of operation.

Before and after the degradation test conducted at BMW, as shown in Figure 8 (see experimental protocol 2 in section 3.2), polarisations curves were obtained in air and O_2 at 80 °C and 100% RH and 2.3 bara. The stoichiometry of the H_2, air and O_2 was 1.5, 2.0 and 9.0 respectively. The polarisation curve obtained before the degradation test is denoted as BOL, while the polarisation curve after the degradation test as EOL. The performance loss for both air and O_2 curves between BOL and EOL depicted in Figure 9, is ~100 mV at 0.5 A/cm^2. The loss of 100 mV after only 60 hours of operation is very high, even though the HFR value decrease over this period. The origin of the HFR reduction during the degradation test is not clear at the moment, however it cannot be correlated to the hydration of the MEA as the HFR was stable after the conditioning period and before the start of the degradation test. It may relate to increasing saturation of catalyst layer ionomer with water.

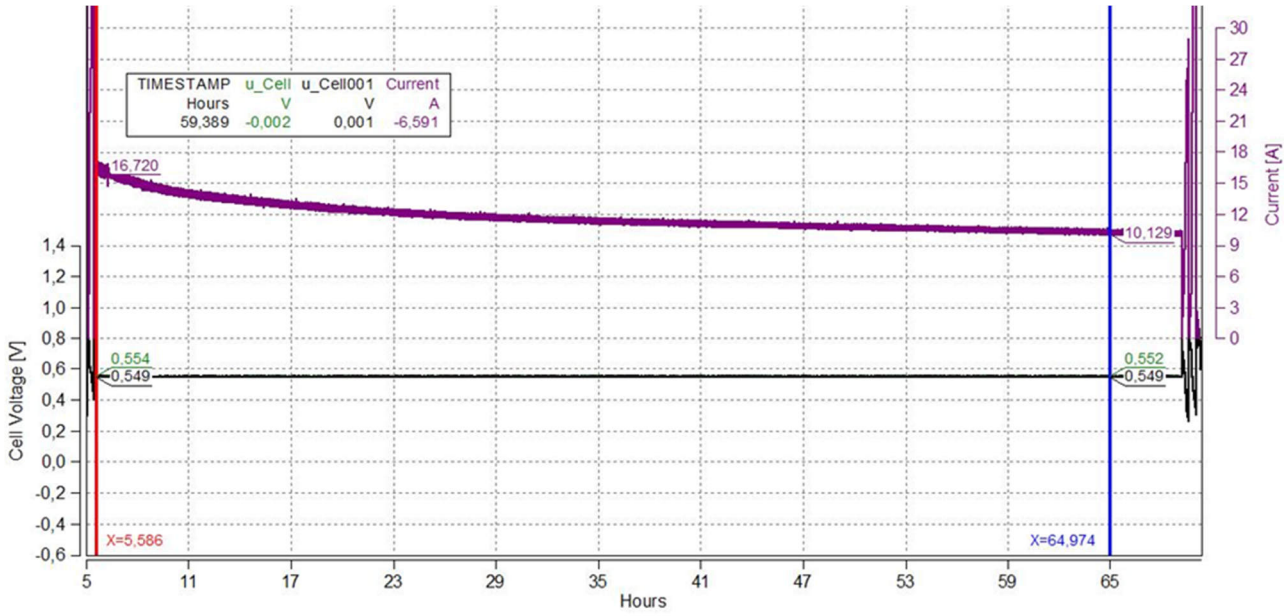

Figure 8. Stability test conducted at BMW at 0.55 V under 100% RH and 2.3 bara with a cell temperature 80 °C under stoichiometry of 1.5 for H_2 and 2.0 for air.

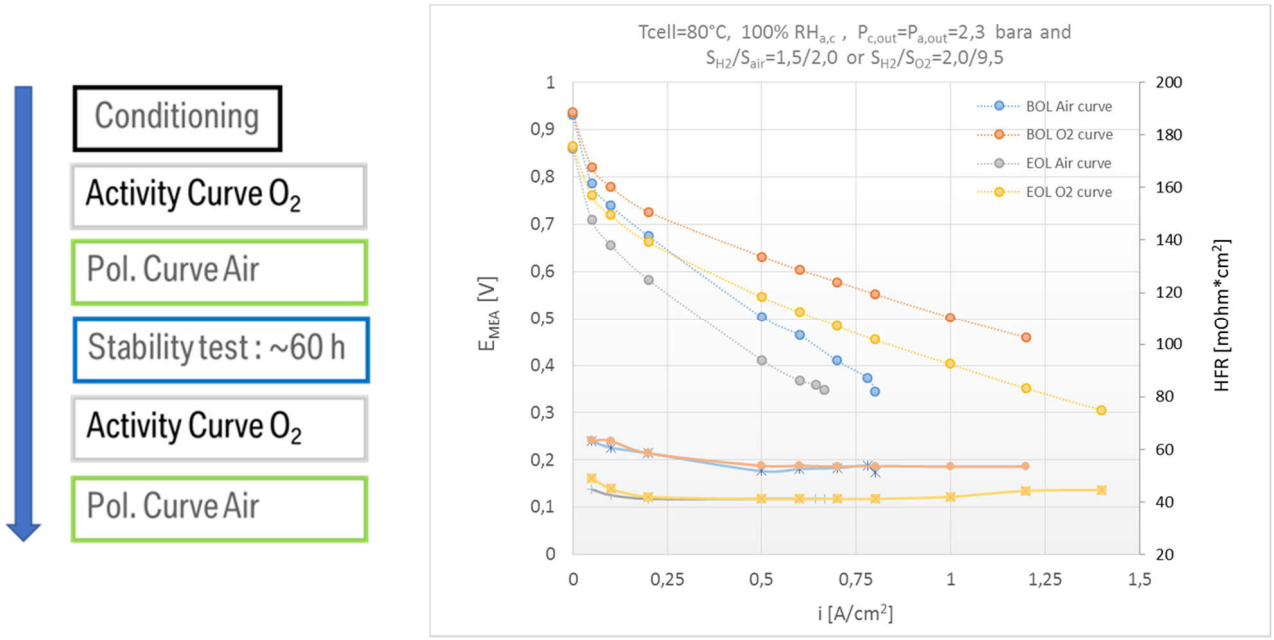

Figure 9. Performance curves under 100% RH and 2.3 bara under H_2 and O_2 stoichiometry of 2.0 and 9.5 respectively as well as H_2 and air stoichiometry of 1.5 and 2.0 respectively. The polarisation curves were acquired before the stability test (BOL) and after the stability test (EOL).

Similar behaviour was observed by JMFC regarding the degradation rate and profile, Figure 10.

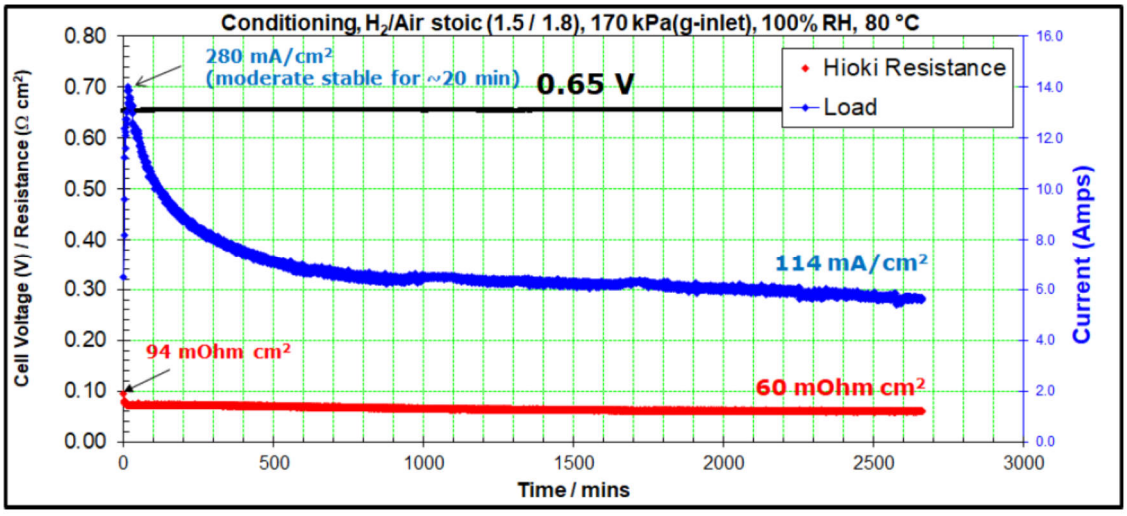

Figure 10. Stability test of Pajarito Powder CCMs at JMFC at 100% RH and 170 $kPa_{,gauge\text{-}inlet}$ under H_2 and Air stoichiometry of 1.5 and 1.8 respectively, under constant voltage 0.65 V. Overview of 45 hours of holding at 0.65 V.

3.3 Stoichiometry and Pressure Sensitivity of Cathodic Electrode

The sensitivity of performance of the MEA with respect to air stoichiometry and pressure was investigated by BMW. Table 4 and 5 show the experimental conditions as well as the obtained results.

Table 4. Cathode stoichiometry dependence of the Pajarito Powder CCMs at 0.5 A/cm^2 and 100% RH and 80 °C under 2.3 bara.

Duration					Stoich		Gas temperature (°C)		Pressure (kPa Abs)		Humidification		Coolant	
	Current Density (A/cm^2)	Voltage (V)	V_{MEA} (V)	HFR-R_{BP} (mohm*cm^2)	H_2	Air	H_2	Air	H_2 out	Air out	H_2 dew point (°C)	Air dew point (°C)	Flowrate (L/min)	Temp. in (°C)
5 min	0.500	0.508	**0.532**	**41.2**	2	**2**	90	90	230	230	80	80	1.5	80
5 min	0.500	0.493	**0.517**	**41.2**	2	**1.8**	90	90	230	230	80	80	1.5	80
5 min	0.500	0.485	**0.509**	**41.2**	2	**1.7**	90	90	230	230	80	80	1.5	80
5 min	0.500	0.472	**0.496**	**41.2**	2	**1.6**	90	90	230	230	80	80	1.5	80
5 min	0.500	0.452	**0.476**	**41.2**	2	**1.5**	90	90	230	230	80	80	1.5	80
5 min	0.500	0.430	**0.454**	**41.2**	2	**1.4**	90	90	230	230	80	80	1.5	80

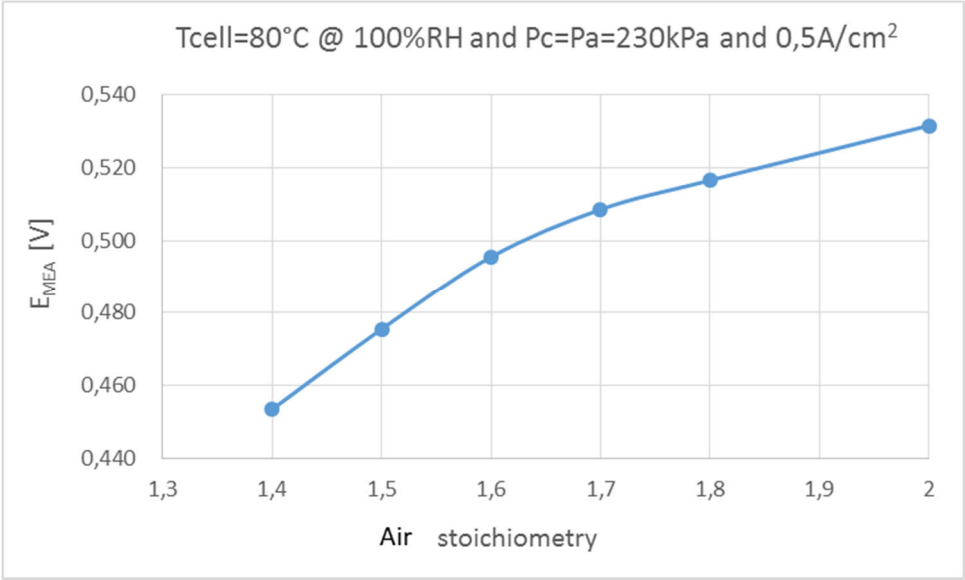

Figure 11. Air stoichiometry sensitivity at 0.5 A/cm^2 under 100% RH and 2.3 bara with a cell temperature 80 °C under stoichiometry of 2.0 for H_2 and 1.4-2.0 for air.

It is clear from Figure 11, that the Pajarito Powder CCMs exhibited a very large air stoichiometry sensitivity. This could be attributed to the thickness of the cathode catalyst layer, which has been estimated to be ~100 µm based on the packing density of the Fe-N-C Pajarito Powder catalyst and the catalyst loading. Another possible explanation could be inhomogeneous ionomer distribution or too high I/C ratio, blocking and flooding the pores of the electrodes under 100% RH. The above hypothesis could also explain the pressure sensitivity results: as shown in figure 12, there is no significance influence of the cathode pressure on the MEA performance. As no information is given regarding the catalyst layer composition from Pajarito Powder (EWii manufactured), we can only speculate.

Table 5. Cathode pressure dependence of the Pajarito CCMs at 0.5 A/cm^2 and 100% RH and 80 °C under 2.3 bara.

Duration					Stoich		Gas temperature (°C)		Pressure (kPa Abs)		Humidification		Coolant	
	Current Density (A/cm^2)	Voltage (V)	V_{MEA} (V)	HFR-R_{BP} (mohm*cm^2)	H_2	Air	H_2	Air	H_2 out	Air out	H_2 dew point (°C)	Air dew point (°C)	Flowrate (L/min)	Temp. in (°C)
5 min	0500	0.443	0.467	36.46	1.5	1.8	90	90	190	170	80	80	1.5	80
5 min	0.500	0.454	0.478	36.46	1.5	1.8	90	90	190	190	80	80	1.5	80
5 min	0.500	0.446	0.470	36.46	1.5	1.8	90	90	190	200	80	80	1.5	80
5 min	0.500	0.454	0.478	36.50	1.5	1.8	90	90	190	230	80	80	1.5	80
5 min	0.500	0.457	0.481	36.46	1.5	1.8	90	90	190	250	80	80	1.5	80

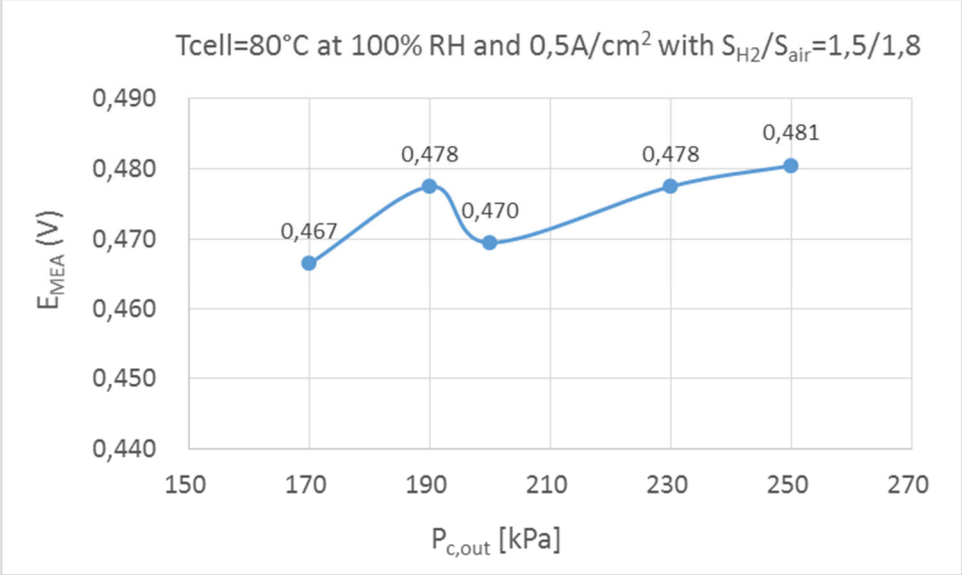

Figure 12. Cathode pressure sensitivity at 0.5 A/cm^2 under 100% RH and 1.9 bara at the anode with a cell temperature 80 °C under stoichiometry of 1.5 for H_2 and 1.8 for air, while the cathode pressure varies from 1.7-2.5 bara.

In order to ensure that during our testing for the cathode air stoichiometry and pressure sensitivity the MEA has not degraded too much, such that it would compromise the recorded data, polarisation curves were obtained during different stages of the testing procedure. Figure 13 shows a schematic representation of the experimental procedure for cathode air stoichiometry and pressure sensitivity tests. From the data depicted in Figure 13b, it is clear that even after 6 hours of operation the MEA exhibits significant performance loss; thus, for sensitivity tests with this kind of MEA the evaluation should be conducted within 3-4 hours of the activation procedure.

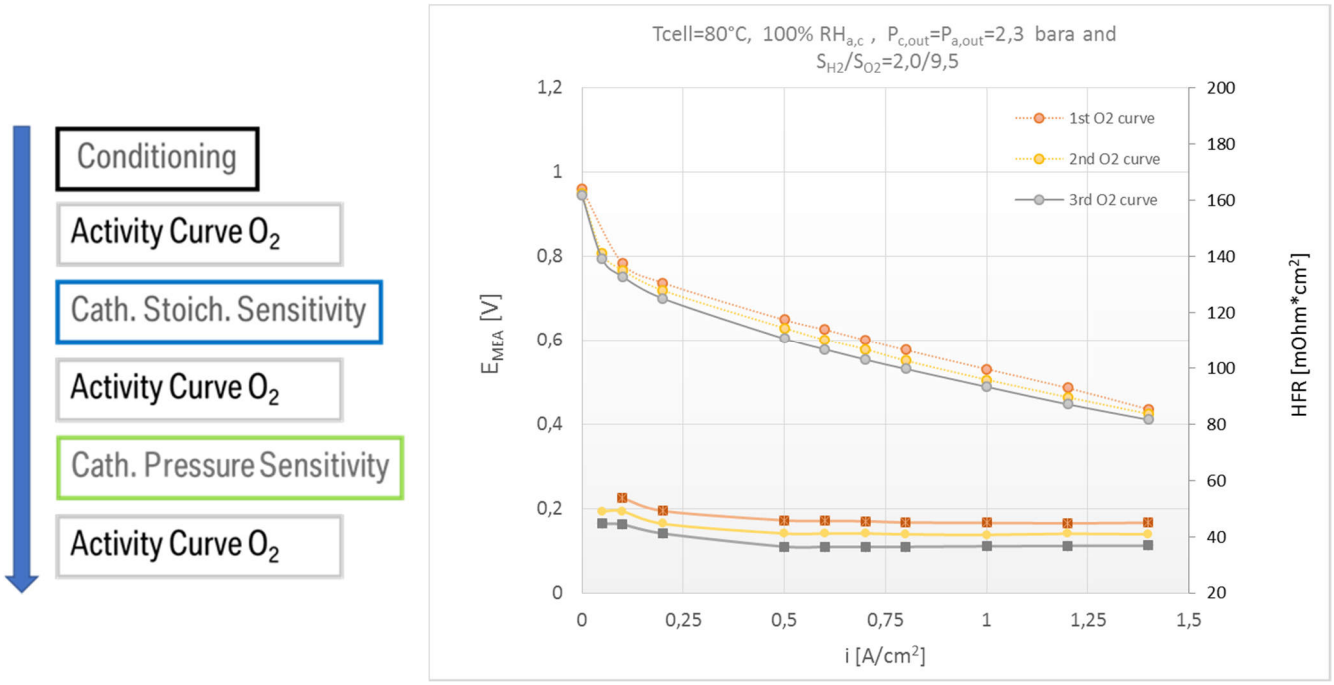

Figure 13 a. Schematic representation of the experimental procedure for cathode air stoichiometry and pressure sensitivity tests. b. Performance curves obtained under 100% RH and 2.3 bara under H_2 and O_2 stoichiometry of 2.0 and 9.5 respectively. The polarisation curves were acquired at different stages of the lifetime of the MEA: 1st polarization curve after conditioning, 2nd polarization curve after the air stoichiometry sensitivity and 3rd polarization curve after the pressure sensitivity test.

3.4 Performance of Pajarito Powder CCMs: dry vs wet operating conditions

MEAs received from EWii using Pajarito Powder catalysts were tested with JM 50 cm^2 single cell hardware. Figure 14 shows the performance obtained under wet (upper graph) and dry (lower graph) humidity. The graph shows the performance when the cathode gas was oxygen, helox or air. The use of these three gases are useful to gain better understanding of the catalyst layer performance. The polarisation curves show that this MEA is capable of 0.57 V and 0.43 V at 0.5 A/cm^2 in oxygen and air respectively. The membrane resistance measured at 100% RH was 57 Ohm.cm^2 which is in line with a good proton conducting membrane at this humidity. The iR free oxygen performance is shown as a red dashed line in Figure 14.

It is interesting to observe that the polarisation curve in H_2/Air and H_2/helox gives a straight line with a loss due to an ohmic resistance. In other words, it does not show a typical mass transport loss with a curvature at higher currents. The blue star overlaid in Figure 14 represents the maximum voltage recorded at 280 mA/cm^2, which was measured at 0.65 V, H_2/Air. This shows the potential performance of this layer and the data suggest that the cathode layer tends to accumulate water with time. The yellow star in Figure 14 shows the performance reported by Pajarito Powder in H_2/Air, which is 150 mV higher than the performance obtained with the JM protocol and hardware.

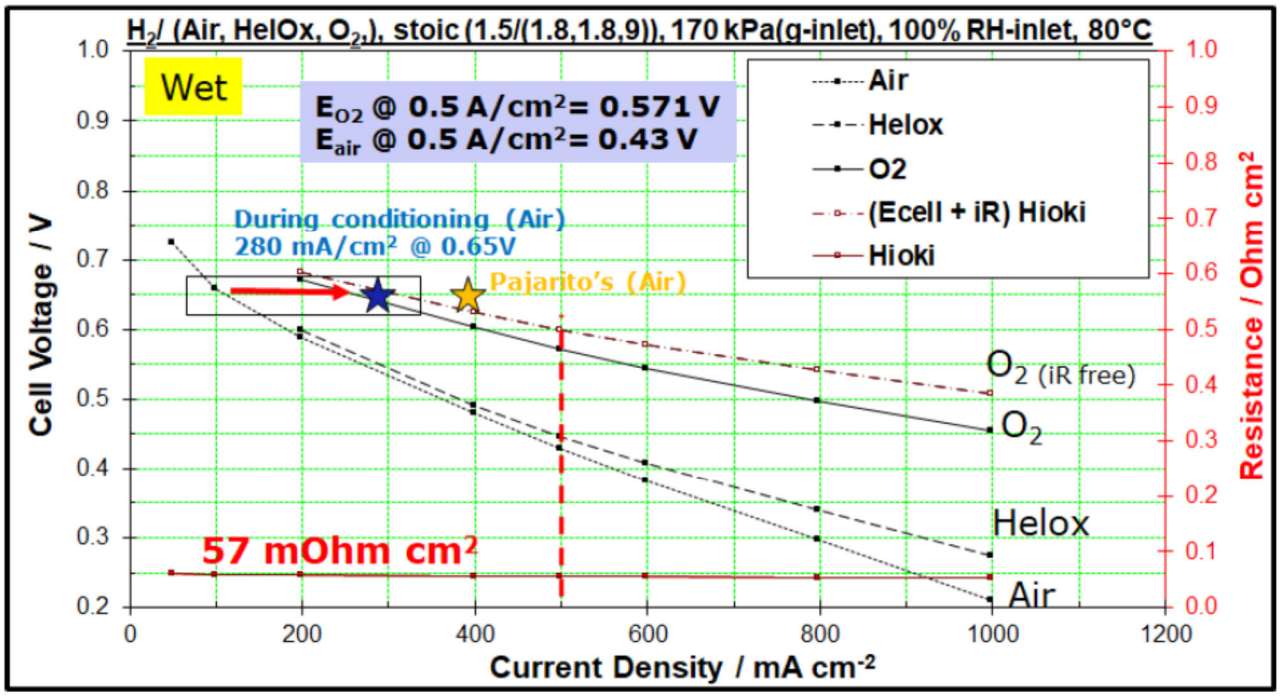

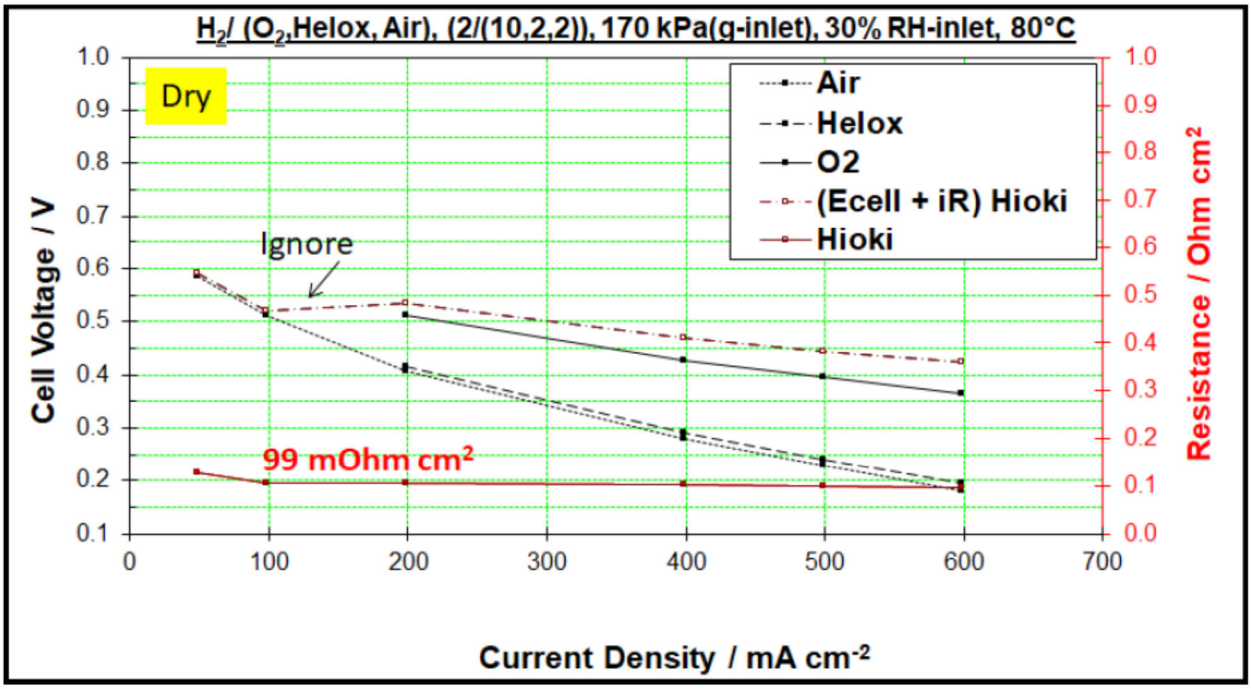

Figure 14. Polarisation curves in 50 cm^2 single cells under H_2/O_2 /Helox/Air at 80°C, 170 kPa-g inlet and 100% (upper graph) and 30% RH (lower graph).

In order to gain a better understanding of the performance losses, Figure 15, upper graph, shows the oxygen and helox gains. This plot shows very high oxygen gains from 0.4 A/cm^2 onwards, which is indicative of a water-rich catalyst layer where a high proportion of the catalytic sites are severely occluded by water. For comparative purposes, a Pt/C state of the art catalyst layer will have an oxygen gain of ~40

mV up to 1.5 A/cm^2. The helox gains, although higher than a standard Pt/C layer, are not as elevated as the oxygen gains, compared to a Pt/C layer. This data indicates that water accumulated in small pores is not easily by-passed in the gas phase; in other words, faster gas-phase diffusion cannot circumvent the pathways blocked by liquid water.

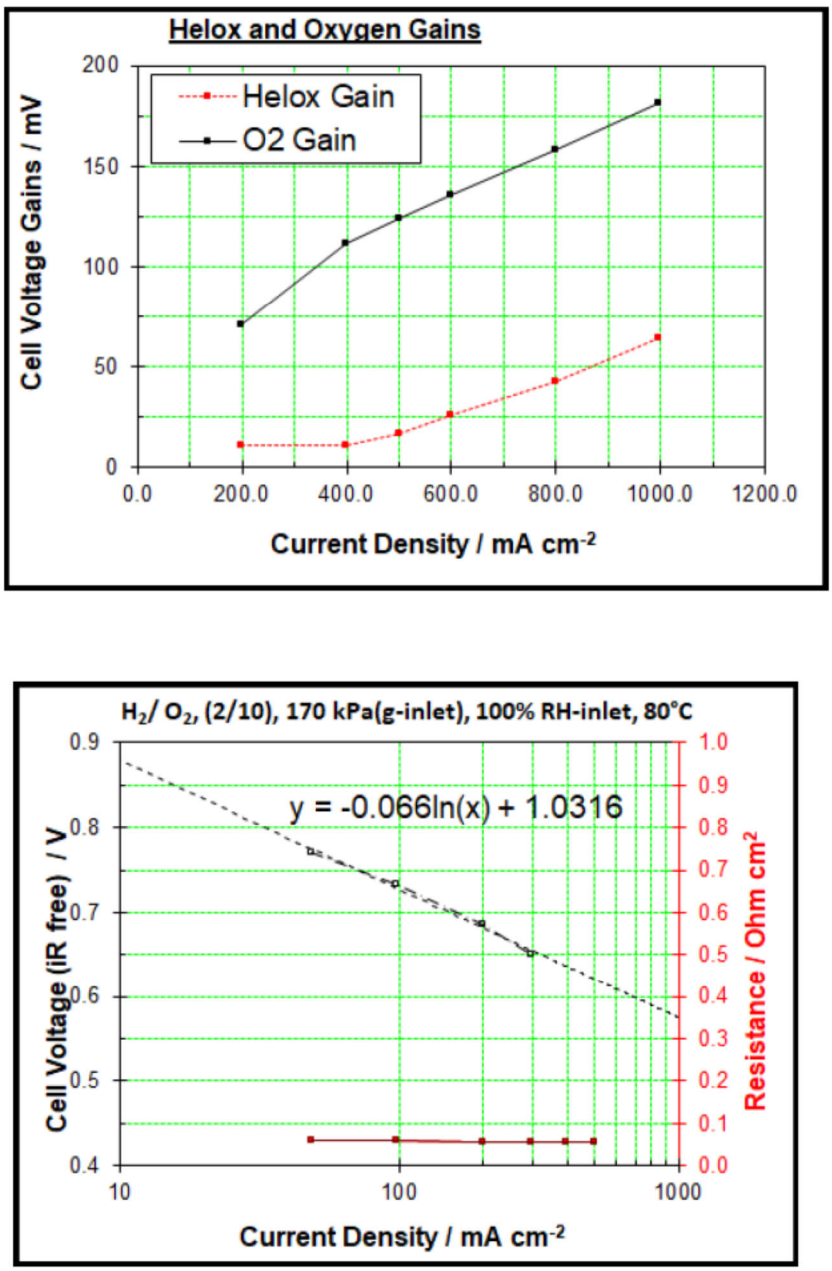

Figure 15. Upper plot shows the oxygen and helox gains obtained for performance data shown in Figure 14. Lower plot shows a Tafel plot (iR free) under H_2/O_2 from figure 14.

On the other hand, the lower graph in Figure 15 shows a Tafel plot in H_2/O_2 with a slope of 66 mV/dec which is the same value as a Pt/C catalyst and could be related to similar rate-limiting step for the oxygen reduction reaction as on Pt.

During the course of this work, a call with Pajarito Powder was organised to discuss the reasons for lower performance obtained at JM. Pajarito kindly shared the results of this type of cathode catalyst and Figure 16 shows performance data in 50 cm^2 single cells received from Pajarito Powder's own testing. Polarisation curves in red and green represent performance in H_2/O_2 under wet (100% RH) and dry (32% RH) conditions. The data obtained at JM with MEAs provided by EWii are shown in the same figure by the solid black line (100 %RH) and the dashed black line (30% RH). The results show that the performance obtained with JM hardware is lower compared to Pajarito Powder's hardware under wet conditions, but significantly better under dry conditions. Due to the differences in MEA components, conditioning and test protocols and hardware it is not possible to identify the origin of the differences observed. Although the samples use the same type of Fe-N-C cathode the MEA configuration is not identical and this plot is used for reference only.

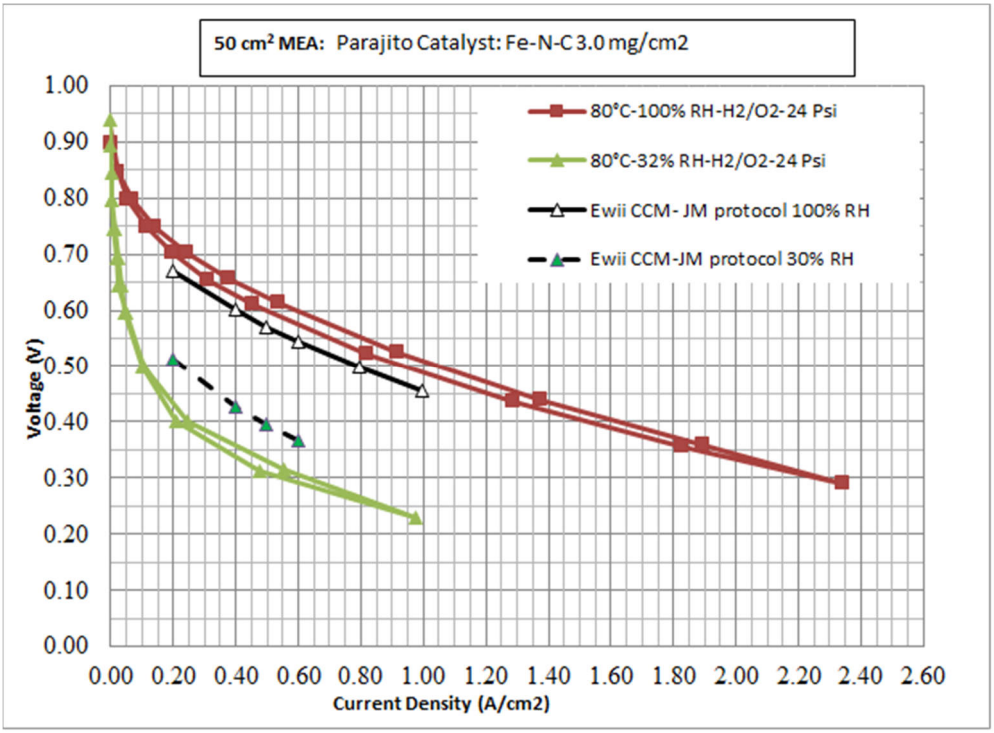

Figure 16. Polarisation curves in 50 cm^2 single cells under H_2/O_2 and H_2/air at 80 °C and 100 and 30% RH. Red and green lines represent the performance obtained by Pajarito Powder using their hardware. Solid and dashed lines represent the performance obtained at JM using EWii MEAs.

3.5 Performance of Pajarito Powder CCMs at 4 different operating points

The electrochemical performance targets at the key operating points for the single cell are shown in Table 6. Table 6 contains an initial target as well as the achieved performance at each operating mode with the Pajarito Powder CCMs. The results depicted in Table 5 were obtained at BMW. The CCMs were not able to achieve the expected performance targets for any operating point. Based on the results presented in previous sections, the origin of the poor performance for these particular MEAs could be attributed to the following reasons:

1. The proton exchange membrane is too thick and thus causes very large ohmic losses at high current densities, especially under dry operating conditions.

2. The cathode electrode thickness is too high causing large mass and proton transport limitations in the catalyst layer, in addition to water management issues.
3. The I/C in the catalyst layer is too high, thus blocking the pores of the already thick catalyst layer hindering further mass transport.

Table 6. Performance key operating modes conditions and performance requirements, as well as achieved voltage and current densities from the commercial Pajarito Powder CCMs .

Specifications	Unit	Mode 1	Mode 2	Mode 3	Mode 4
Current density target	A/cm^2	0.1	1.4	0.6	0.6
Achieved Current density	A/cm^2	0.1	0.2	0.15	0.3
Actual MEA voltage	V	0.602	0.382	0.418	0.403
Required cell voltage	V	0.75	0.3	0.71	0.7
HFR	$mohm*cm^2$	106.2	113.0	122.1	79.7
Cell temperature in	°C	65	90	90	80
Anode					
Pressure anode inlet	bara	2.3	2.3	2.3	2.5
H_2 concentration anode (dry)	mol%	100	100	100	100
N_2 concentration anode (dry)	mol%	0	0	0	0
Dew point anode inlet	°C	45	65	65	63.8
RH anode inlet	%	38.5	35.7	35.7	50
Stoichiometry H_2		1.4	1.4	1.4	1.3
Cathode					
Pressure cathode inlet	Bara	2.3	2.3	2.3	2.3
O_2 concentration cathode (dry)	mol%	21	21	21	21
N_2 concentration cathode (dry)	mol%	79	79	79	79
Dew point cathode inlet	°C	45	65	65	53
RH cathode inlet	%	38.5	35.7	35.7	30
Stoichiometry Air		1.8	1.8	1.8	1.5

3.6 Comparison of performance of commercial Pajarito Powder CCM between BMW-JMFC-CNRS

In order to investigate the reproducibility of the testing amongst the partners on the performance of the commercially available Fe-N-C based MEAs, we compared the data obtained at BMW-CNRS-JMFC. Figure 18 depicts the voltage of the MEAs as measured at 0.5 A/cm^2 in the different screener single cell hardwares. The highest performance was obtained at BMW. The observed differences in performance

can be attributed to the different hardware and compression of the MEA during testing, as well as different activation protocols.

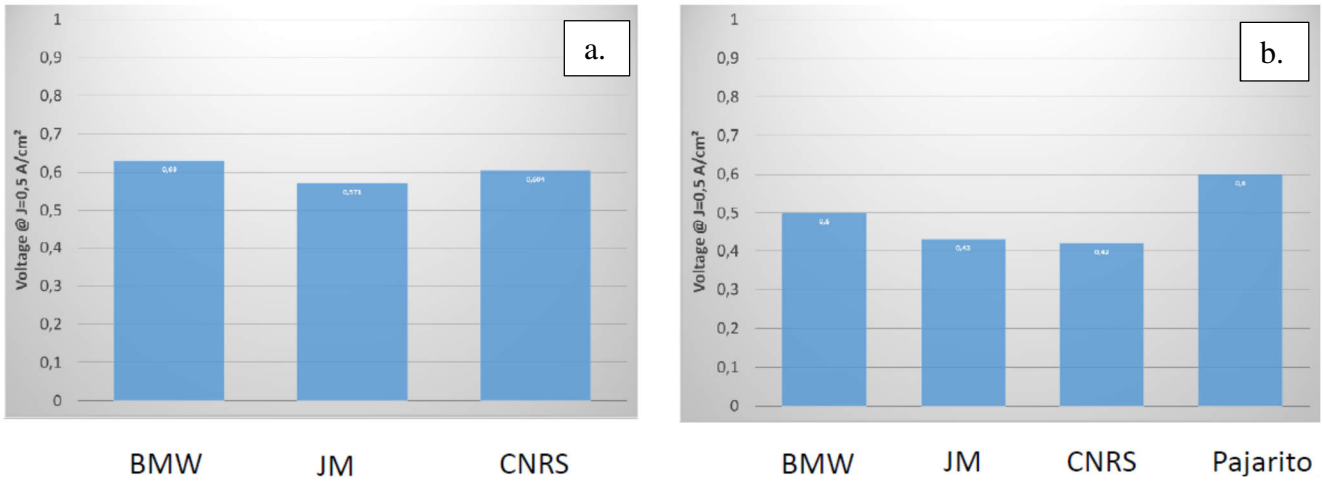

Figure 17. Performance comparison at 0.5 A/cm^2 under 100% RH and 2.3 bara under a. H_2 and O_2 stoichiometry of 2.0 and 9.5 respectively and b. H_2 and air stoichiometry of 1.5 and 2.0 respectively.

In Figure 17b we also show for comparison the performance reported from Pajarito Powder for the same type of MEA. The MEA measured by Pajarito Powder exhibits almost 100 mV better performance compared to the highest recorded performance by CRESCENDO partners. This can be attributed to different hardware configurations as well as differences in the measurement process. Another explanation might be that the polarisation curve from Pajarito Powder was recorded under slow scan rate and not under constant load as in our case. In our case, the holding time per measurement point was 5 min with a sampling of 30 sec; earlier recording of data points after stepping to a new current density can lead to significantly higher voltages. However, these differences in performance, shows challenges on comparing results on PGM-free based MEAs.

3.7 EX SITU ELECTROCHEMICAL CHARACTERISATION RESULTS (RRDE)

The RRDE experiments were performed on two different catalyst loadings on the disk, at 0.2 and 0.8 mg cm^{-2}. Figure 18 shows an example of polarisation curves of the tested catalysts at the higher loading. Measurements were made on the CNRS catalyst before and after ball milling. The smaller particle size appeared to influence the performance of the catalyst in RRDE testing. Figure 19 shows the production of hydrogen peroxide in the potential range from 0.00 – 0.85 V_{RHE}.

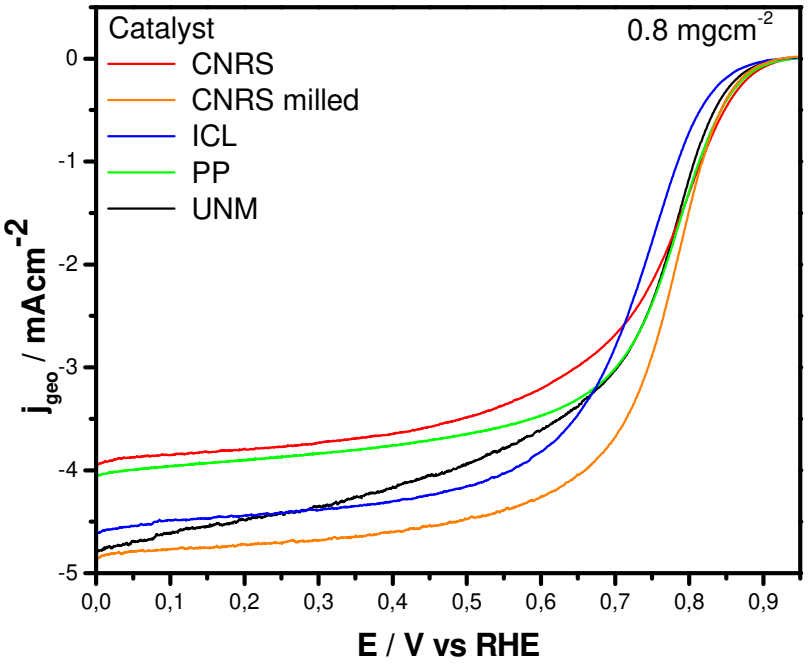

Figure 18. Example of polarisation curves of the catalysts in oxygen-saturated 0.5 M H_2SO_4 at a catalyst loading of 0.8 mg cm^{-2}.

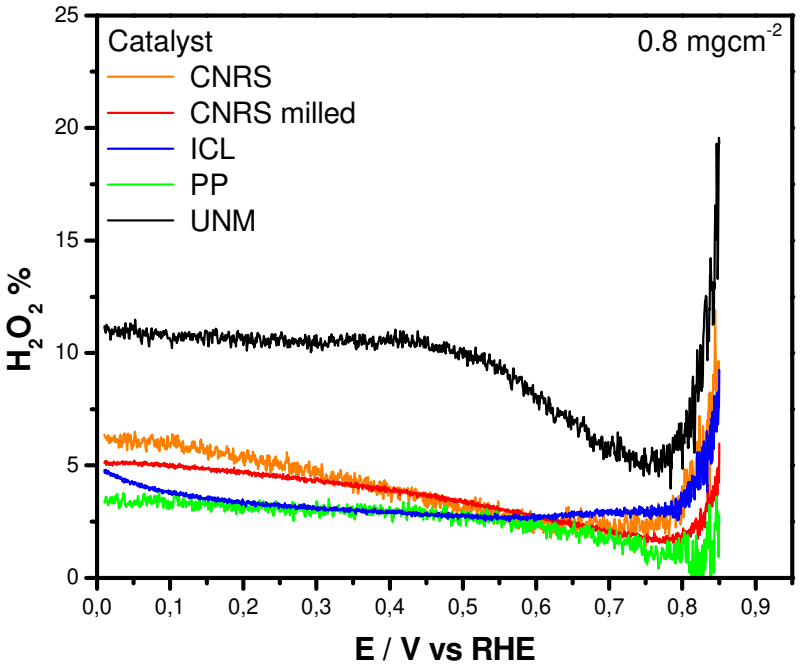

Figure 19. Example of determined H_2O_2 production of the tested catalysts in oxygen-saturated 0.5 M H_2SO_4 at a catalyst loading of 0.8 mg cm^{-2}.

Table 7 and
Table 8 show the averaged values of the main electrochemical data with their corresponding errors. Each catalyst was measured in at least two different laboratories with two to three repetitions for each catalyst and loading. Hence the error bars correspond to the standard deviation of the average values between different laboratories.

Table 7: Electrochemical metrics at catalyst loading of 0.2 mg cm^{-2}.

0.2 mg cm^{-2}					
Catalyst	J_{Lim}	J_{Kin}	J_{Kin}	H_2O_2	H_2O_2
	(0.2 V_{RHE}) [mA cm^{-2}]	(0.80 V_{RHE}) [mA cm^{-2}]	(0.85 V_{RHE}) [mA cm^{-2}]	(0.2 V_{RHE}) [%]	(0.7 V_{RHEE}) [%]
CNRS	3.5 ± 0.3	0.40 ± 0.09	0.12 ± 0.06	5 ± 2	5 ± 3
ICL	4.77 ± 0.07	0.24 ± 0.06	0.05 ± 0.02	8 ± 6	14 ± 9
PP	4.3 ± 0.6	0.465 ± 0.005	0.100 ± 0.001	6 ± 4	7 ± 3
UNM	3.9 ± 0.7	0.48 ± 0.43	0.10 ± 0.09	7 ± 5	8 ± 5

Table 8: Electrochemical metrics at catalyst loading of 0.8 mg cm^{-2}.

0.8 mg cm^{-2}					
Catalyst	J_{Lim}	J_{Kin}	J_{Kin}	H_2O_2	H_2O_2
	(0.2 V_{RHE}) [mA cm^{-2}]	(0.80 V_{RHE}) [mA cm^{-2}]	(0.85 V_{RHE}) [mA cm^{-2}]	(0.2 V_{RHE}) [%]	(0.7 V_{RHE}) [%]
CNRS	4.3 ± 0.5	1.8 ± 1.0	0.5 ± 0.3	5 ± 4	4 ± 6
ICL	4.41 ± 0.03	0.81 ± 0.01	0.18 ± 0.01	3.0 ± 0.3	3.4 ± 0.6
PP	4.4 ± 0.5	2.6 ± 0.7	0.7 ± 0.2	2.6 ± 0.6	1.9 ± 0.3
UNM	4.9 ± 0.3	2.1 ± 1.2	0.4 ± 0.2	5 ± 4	3 ± 2

Table 9**:** Initial mass based kinetic current at the two different loadings and potentials shows the comparison of mass-based current for each catalyst at loadings of 0.2 and 0.8 mg cm^{-2}. Due to the error margin, a precise comparison of the catalysts is not easily achievable, but Catalyst 3 from Pajarito Powder (PP) shows the highest initial kinetic current at both potentials at 0.8 mg.cm^{-2}. At 0.2 mg.cm^{-2}, the UNM material is marginally higher.

Table 9: Initial mass based kinetic current at the two different loadings and potentials.

Catalyst	$J_{Kin,mass}$ 0.80 V_{RHE}		$J_{Kin,mass}$ 0.85 V_{RHE}	
	0.2 mg cm^{-2}	0.8 mg cm^{-2}	0.2 mg cm^{-2}	0.8 mg cm^{-2}
	[mA mg^{-1}]	[mA mg^{-1}]	[mA mg^{-1}]	[mA mg^{-1}]
CNRS	2.0 ± 0.4	2.2 ± 1	0.6 ± 0.3	0.7 ± 0.4
ICL	1.2 ± 0.3	0.7 ± 0.5	0.26 ± 0.09	0.22 ± 0.01
PP	2.33 ± 0.02	3.2 ± 0.9	0.496 ±0.003	0.9 ± 0.3
UNM	2.4± 2	2.60 ± 1	0.5 ± 0.5	0.6 ± 0.2

The summary results of Tables 7-8 show that the commercial Fe-N-C catalyst, labelled PP, performs closely similarly to the other laboratory catalysts in terms of activity at 0.8 or 0.85 V_{RHE}, and also in terms of amount of peroxide released during the ORR. The main difference is in its Fe speciation, with the PP catalyst having a higher relative content of metallic and metal-carbide Fe particles compared to the other catalysts. Since the PP catalyst was prepared via HF leaching after the pyrolysis, it can be assumed that the particles are well embedded in N-doped carbon shells, and this should prevent excessive Fe leaching during RRDE or PEMFC testing. The AST in RRDE (5 000 cycles in load-cycling mode) reported in D3.1 shows, however, a significant decrease of ORR activity for the PP and UNM materials (both prepared via silica templating), not observed for the catalysts from CNRS and ICL.

In summary, the PP commercial catalyst is, from RRDE studies, seen to be similar, in terms of initial activity and selectivity, to other best-in-class Fe-N-C laboratory catalysts, used for MEA benchmarking and sensitivity testing.

4. CONCLUSIONS AND FUTURE WORK

As shown in the RRDE section, the more promising material for MEA testing was the Pajarito Powders (PP) Fe-N-C catalyst, although this ignores stability criteria. The PP catalyst exhibited higher yield in terms of H_2O_2 decomposition under 0.8 mg/cm^2 compared to 0.2 mg/cm^2. This is to be expected as thicker catalyst layers results in the increase of the residence time of the H_2O_2 in the catalyst layer, and thus yields in higher conversion rates of H_2O_2 towards H_2O. As PP showed the lower H_2O_2 formation at thick electrodes, this material was considered the most promising for fuel cell testing: the PGM-free based electrodes are generally thick in the range of 40-100 µm (i.e 0.8-3mg/cm^2) and thus similar behaviour was expected in terms of H_2O_2 formation.

However, since we had already received an optimised and commercially available CCM containing the same PP catalyst that was tested in RDE, there was no need in manufacturing and optimising CCMS in the partners' laboratory in this work package. Thu,s only the commercial Pajarito Powder CCMs were benchmarked in fuel cells. From the obtained results, it was clear that these MEAs do not meet the performance and stability target requirements of this project.

It has to be stated that even though in RRDE the PP catalysts showed very promising performance, the transfer of the performance in fuel cell is not straightforward. One of the major origins of the performance difference arises from significant mass transport and proton conduction resistance in the catalyst layer of a MEA, as a result of the higher catalyst loading compared to RRDE.

However, testing these MEAs under different operating conditions gave us valuable insights on what needs to be changed for the next generation Fe-N-C CCMs under development in CRESCENDO:

1. The membrane needs to be thinner, preferably between 10-15 µm in order to meet automotive operation requirements.
2. The catalyst layer thickness needs to be significantly reduced, with a target of below 40 µm.
3. The I/C ratio needs to be adjusted in order not to block the mesoporous structure of the electrode, but without sacrificing the proton conductivity in the catalyst layer under dry operating conditions.
4. A catalyst with significantly higher ORR activity is needed and with significantly higher durability.